

# Enhancing Targeted Radiotherapy by Copper(II)diacetyl-bis( $N^4$ -methylthiosemicarbazone) Using 2-Deoxy-D-Glucose<sup>1</sup>

Rebecca L. Aft,<sup>2</sup> Jason S. Lewis, Fanjie Zhang, Joonyoung Kim, and Michael J. Welch

Department of Surgery [R. L. A., F. Z.], Mallinckrodt Institute of Radiology [J. S. L., J. K., M. J. W.], and Alvin J. Siteman Cancer Center [R. L. A., J. S. L., M. J. W.], Washington University School of Medicine, and John Cochran Veterans Administration Hospital [R. L. A.], St. Louis, Missouri 63110

## ABSTRACT

Most cancer deaths are a consequence of resistance to conventional chemotherapy and radiation therapy. This may be attributable to unique phenotypic characteristics of solid tumors. We have exploited two well-described characteristics of solid tumors commonly associated with treatment failure, high glucose use and hypoxia, to design a unique therapy based on the selective accumulation of two cytotoxic compounds, 2-deoxyglucose (2-DG) and copper(II)diacetyl-bis( $N^4$ -methylthiosemicarbazone) ( $^{64}\text{Cu}$ -ATSM).  $^{64}\text{Cu}$ -ATSM localizes to hypoxic regions of tumors and has been used for administering a high local dose of radiation therapy after uptake by cells. 2-DG, a glucose analog, selectively accumulates in cancer cells and interferes with energy metabolism, resulting in cancer cell death. 2-DG has been shown to potentiate the cytotoxic effect of ionizing radiation and certain chemotherapeutic agents. We have tested the effect of 2-DG on tumor response when combined with  $^{64}\text{Cu}$ -ATSM in a mouse breast tumor model using the highly aggressive mouse mammary carcinoma cell line EMT-6. 2-DG administered up to 2 mg/g of body weight daily resulted in no weight loss or systemic symptoms. EMT-6 mammary tumors had similar uptake of [ $^{18}\text{F}$ ]fluoro-2-deoxyglucose before and after 2 weeks of 2-DG treatment as determined by microPET imaging, indicating that resistance to 2-DG uptake does not develop. Pretreatment of tumor-bearing mice with 2-DG resulted in increased uptake of  $^{64}\text{Cu}$ -ATSM by tumors compared with nontreated mice. This effect was not observed with the nonhypoxia-specific agent copper(II)pyruvaldehyde-bis( $N^4$ -methylthiosemicarbazone). When 2-DG was combined with a single dose of  $^{64}\text{Cu}$ -ATSM (2 mCi), tumor growth was inhibited ~60% compared with untreated mice, and animals survived ~50% longer than untreated mice or animals treated with each agent alone (32 versus 20 days). The maximum effect on tumor growth and survival was observed when 2-DG was administered daily for the lifetime of the mouse. Our results indicate that 2-DG potentiates the effect of  $^{64}\text{Cu}$ -ATSM on tumoricidal activity and animal survival. We hypothesize that 2-DG alters the metabolic state of the cell, leading to increased uptake of  $^{64}\text{Cu}$ -ATSM by the tumor. This would result in a higher local dose of radiotherapy. The continued presence of 2-DG would then prevent the repair of damaged cells, leading to inhibition of tumor growth. Our data indicate that the strategy of combining tumor-specific cytotoxic agents that function by differing mechanisms can result in an effective, selective, tumor-specific cell death with minimal effect on the host.

## INTRODUCTION

Breast cancer is the most common malignancy diagnosed in American women and is currently the second most frequent cause of cancer death despite early detection and treatment. Progression of disease is the result of treatment failure, which is a consequence of resistance to

conventional therapy. Resistance to chemotherapy and radiation therapy may be attributable to phenotypic characteristics of the cancer cells (1). Multiple strategies have been implemented with varying effectiveness to overcome treatment-refractory cancers including combination chemotherapy with agents differing in mechanism, sensitizers to radiation therapy, and inhibitors of receptors (2–5). In this series of experiments, we have tested the efficacy of combining two tumor-specific cytotoxic agents in a mouse model of breast cancer to develop a targeted therapy for breast tumors.

Human tumors preferentially use glycolysis for energy production, even under aerobic conditions (Warburg effect), although this requires more glucose to generate energy and support synthetic functions (6, 7). Glucose use may represent an important regulatory point in the maintenance of the growth and synthetic activity of malignant cells and suppression of apoptosis (8, 9). Our previous experiments confirm this finding and further demonstrate that functional glucose deprivation achieved using the nonmetabolizable glucose analog 2-DG<sup>3</sup> causes apoptosis in breast cancer cells (10). 2-DG is a structural analog of glucose that selectively accumulates in cancer cells after phosphorylation by hexokinase (Fig. 1A). Selective accumulation of 2-DG has been attributed to several metabolic alterations observed in cancer cells including increased glucose transporter expression, resulting in increased uptake (11–13), increased hexokinase activity, and low phosphorylase activity, resulting in intracellular trapping (14–18). Inhibition of glycolysis by phosphorylated 2-DG, 2-DG-6-phosphate, is thought to occur via inhibition of hexokinase and phosphohexoisomerase (19, 20). Cancer cell death by 2-DG may be through intracellular glucose deprivation, resulting in induction of stress-related proteins (21, 22), the generation of free radicals (23), or inhibition of energy metabolism (22–24). Tumor-bearing animals treated with 2-DG exhibit impairment of local tumor growth (18, 25). Recent clinical trials administering 2-DG in combination with IR to treat brain gliomas indicate that oral 2-DG is well tolerated by patients and may be protective to normal surrounding tissues (26).

$^{64}\text{Cu}$ -ATSM has been used as an imaging agent to delineate hypoxic areas within tumors (27–31) and as an agent for targeted radiotherapy (32, 33).  $^{64}\text{Cu}$ -ATSM is a neutral lipophilic molecule of low molecular weight, high membrane permeability, and low redox potential (Fig. 1B; Ref. 27). It is thought that bioreduction of the  $^{64}\text{Cu}$ (II)-ATSM complex intracellularly leads to the release of  $^{64}\text{Cu}$ (I), which then becomes bound to intracellular macromolecules. This process occurs more readily in hypoxic tissue compared with normoxic tissue (28, 34, 35). Uptake of  $^{60}\text{Cu}$ -ATSM by tumors in cervical cancer patients correlates with patient survival and is similar to results obtained using oxygen electrodes to discriminate hypoxic versus nonhypoxic cervical cancers, supporting the use of  $^{60}\text{Cu}$ -ATSM PET imaging as a method for the clinical evaluation of tumor hypoxia (30). Similar results have been reported recently in patients with lung cancer (31).  $^{64}\text{Cu}$  linked to small, tumor-specific molecules

Received 2/27/03; revised 5/30/03; accepted 6/18/03.

The costs of publication of this article were defrayed in part by the payment of page charges. This article must therefore be hereby marked *advertisement* in accordance with 18 U.S.C. Section 1734 solely to indicate this fact.

<sup>1</sup> This study was supported by an Association of Women Surgeons/Ethicon Grant (to R. L. A.). The Cu-64 therapy work was supported by United States Department of Energy Contract DE-FG02-87ER60212 (to M. J. W.). MicroPET imaging is supported by NIH/National Cancer Institute Small Animal Imaging Resource Program Grant 1 R24 CA83060. The Small Animal Imaging Core is supported by National Cancer Institute Cancer Center Support Grant 1 P30 CA91842. The production of Cu-64 is supported by National Cancer Institute Grant R24 CA86307 (to M. J. W.).

<sup>2</sup> To whom requests for reprints should be addressed, at Washington University, 660 South Euclid Avenue, Campus Box 8109, St. Louis, MO 63110. Phone: (314) 747-0063; Fax: (314) 454-5509; E-mail: afr@msnotes.wustl.edu.

<sup>3</sup> The abbreviations used are: 2-DG, 2-deoxy-D-glucose; IR, ionizing radiation;  $^{64}\text{Cu}$ -ATSM, copper(II)-diacetyl-bis( $N^4$ -methylthiosemicarbazone);  $^{64}\text{Cu}$ -PTSM, copper(II)-pyruvaldehyde-bis( $N^4$ -methylthiosemicarbazone); PET, positron emission tomography; FDG, fluoro-2-deoxyglucose; i.g., intragastric; SUV, standardized uptake value; LET, linear energy transfer.

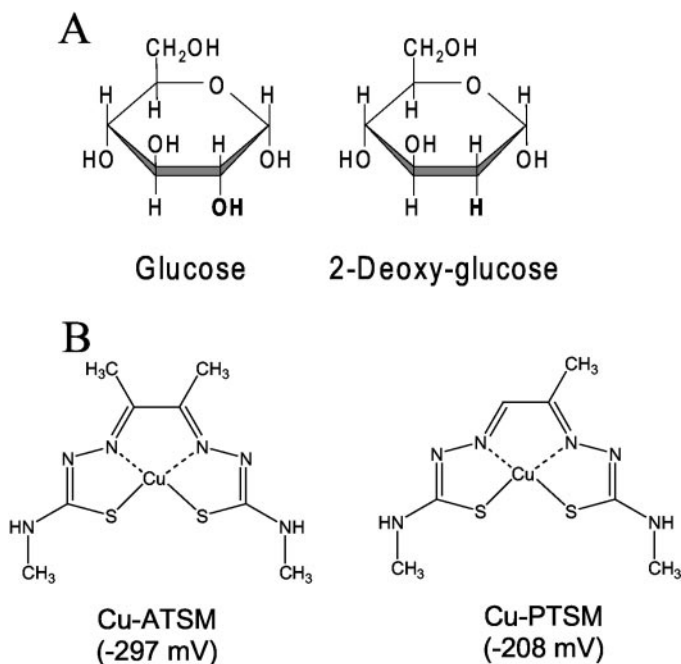


Fig. 1. Structure of 2-DG and Cu-ATSM. A, 2-DG differs from glucose by substitution of hydrogen for a hydroxyl at the 2 position. This prevents further metabolism after phosphorylation to 2-DG-6- $\text{PO}_4$  by hexokinase. B, Cu-ATSM and Cu-PTSM differ by a single methyl group in the bis(thiosemicarbazone) complex. This results in a change in redox potential, which affects biological properties.

has been used as an agent for administering high-dose local radiotherapy. Experiments using  $^{64}\text{Cu}$  linked to monoclonal antibodies, ATSM, or PTSM have demonstrated that  $^{64}\text{Cu}$  can inhibit solid tumor growth and prevent peritoneal spread of cancer cells (32, 36–38). During decay,  $^{64}\text{Cu}$  emits a 0.58-MeV  $\beta$ -particle (40%), a 0.66-MeV  $\beta^+$  particle (19%), and a  $\gamma$  of 1.34 MeV (0.5%), giving a wide variety of potentially radiotoxic emissions. Moreover, during decay by electron capture, the copper radionuclide emits highly radiotoxic Auger electrons with high linear energy transfer, which have a tissue penetration of 0.02–10  $\mu\text{m}$ . Because of the short range and relatively larger linear energy transfer, Auger electrons are potentially more radiotoxic than the higher energy  $\beta$ -particles if localized in the nucleus (39, 40).

Hypoxic tumors are relatively resistant to conventional therapy, and hypoxia is associated with a more aggressive malignant phenotype (41). Tumor hypoxia appears to be a dynamic process dependent on blood flow and tumor vasculature, resulting in areas of acute and chronically hypoxic cells (1). Increased expression of the glucose transporter has been found in areas of relative hypoxia in solid tumors (17). We and others have demonstrated that 2-DG is an effective sensitizer for ionizing radiation (42, 43). 2-DG is thought to act as a radiosensitizer by impairing the ability of the cells to repair damage induced by ionizing radiation (43) or by disruption of thiol metabolism (42). Because of the selective accumulation of 2-DG in cancer cells, increased glucose transporter expression in areas of hypoxia, and synergy with IR, we hypothesized that 2-DG would improve localized radiotherapy with  $^{64}\text{Cu}$ -ATSM, leading to a greater therapeutic response. Our experiments support this hypothesis and furthermore demonstrate that treatment with 2-DG leads to a marked increased uptake and retention of  $^{64}\text{Cu}$ -ATSM by tumors. Treatment of tumor-bearing mice with 2-DG and  $^{64}\text{Cu}$ -ATSM causes inhibition of tumor growth and increased overall survival compared with either treatment alone. From these experimental findings, we propose that administration of 2-DG treatment to tumor-bearing animals results in an alteration in the metabolic state of the tumor, which results in the

increased uptake and retention of  $^{64}\text{Cu}$ -ATSM, resulting in improved overall survival.

## MATERIALS AND METHODS

**Reagents.**  $^{64}\text{Cu}$  was produced on a CS-15 biomedical cyclotron (Cyclotron Corp.) at Washington University using methods reported previously (44, 45). Unless otherwise stated, all chemicals were purchased from Sigma-Aldrich Chemical Co., Inc. (Milwaukee, WI.) All solutions were prepared using distilled deionized water.  $^{64}\text{Cu}$ -ATSM and  $^{64}\text{Cu}$ -PTSM with >98% radiochemical purity were produced by methods described in the literature (27, 46). The compounds were produced at  $1 \times 10^{-2}$  MBq/ $\mu\text{g}$ . [ $^{18}\text{F}$ ]FDG was prepared using the Coincidence Technologies [ $^{18}\text{F}$ ]FDG synthesis module. This method of preparation is based on the methods of Hamacher *et al.* (47).

**Cell Culture.** The mouse mammary tumor line EMT-6 was obtained from the laboratory of Dr. Ronald S. Pardini at the University of Nevada and maintained by serial passage in RPMI1640 containing 10% FCS in a 37°C humidified 95% air, 5%  $\text{CO}_2$  incubator.

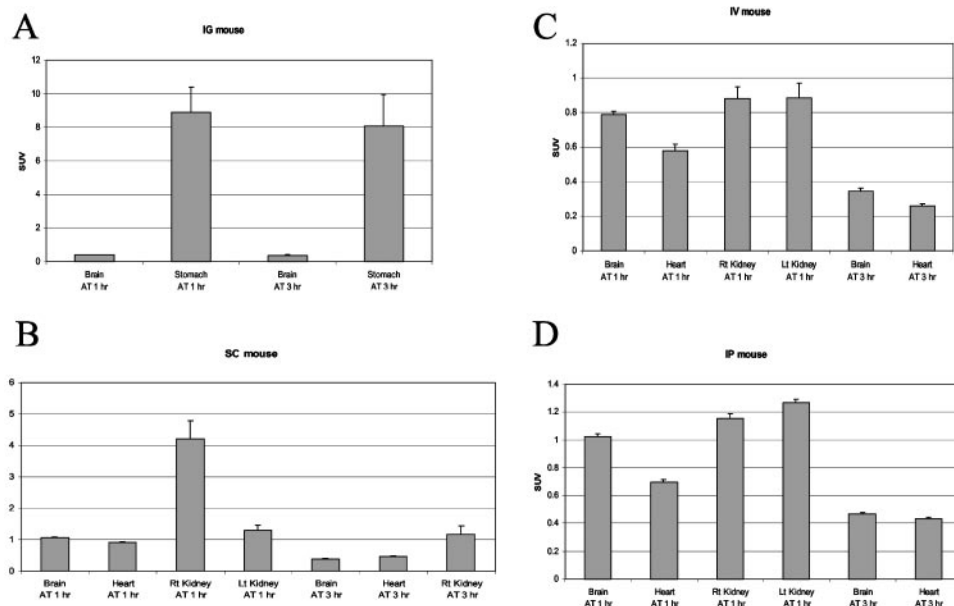
**Animal Models.** All animal experiments were conducted in compliance with the Guidelines for the Care and Use of Research Animals established by Washington University's Animal Studies Committee. BALB/c mice, 5–6 weeks of age, were purchased from Charles River Laboratories (Wilmington, MA). EMT-6 cells ( $2.5 \times 10^5$ ) in 100  $\mu\text{l}$  of 0.9% saline were implanted s.c. into the dorsal flank of each mouse. Four days after implantation when established tumors were palpable (tumors ~0.4–0.5 g), animals were randomized into treatment groups (5–6 animals/group). 2-DG (40 mg/mouse, 2 mg/g of body weight) was injected i.p. daily unless otherwise indicated. For imaging experiments,  $^{64}\text{Cu}$ -ATSM (20 MBq, 500  $\mu\text{Ci}$ ) or  $^{64}\text{Cu}$ -PTSM (20 MBq, 500  $\mu\text{Ci}$ ) was injected into the tail vein. Therapeutic doses of  $^{64}\text{Cu}$ -ATSM or  $^{64}\text{Cu}$ -PTSM (1–2 mCi/mouse) were injected on day 5 into a tail vein or jugular vein. Mice were weighed, and tumor size was measured daily for the first 2 weeks and every second day after that. Tumor volume was calculated as  $(\text{length} \times \text{width} \times \text{height} \times 3.14)/6$ . Data are expressed as the average tumor size or animal weight for each treatment group. Error bars represent the range of measurement. Mice were sacrificed when the tumor reached 10% of the body weight, ulcerated through the skin, or reached 20 mm in greatest diameter. The estimated survival distribution function was generated by a Kaplan-Meier time-to-sacrifice analysis.

**MicroPET Imaging.** PET was performed on a microPET-R4 system (Concorde Microsystems, Inc., Knoxville, TN), which is based on the design of Cherry *et al.* (48). The microPET-R4 has a field view of 8 cm axially by 11 cm transaxially and is capable of spatial resolution of 2.3 mm and an absolute sensitivity of 1020 cps/microcurie in the middle of the field-of-view. Images were generated from three-dimensional sinogram data, rebinned to 2-dimensional format by the FORE algorithm, followed by two-dimensional filtered-back projection (49). For imaging studies on mice bearing EMT-6 tumors, the mice were anesthetized with 1–2% isoflurane before scanning, positioned supine, and immobilized in a custom-prepared cradle. Two mice were imaged side by side and remained in the same bed position for all time points. All imaging was performed in a temperature-controlled imaging suite with close monitoring of the physiological status of the animals.  $^{64}\text{Cu}$ -ATSM or  $^{64}\text{Cu}$ -PTSM was administered i.v. as a bolus injection, followed by 25 min of dynamic data collection ( $20 \times 5$ -s frames,  $6 \times 30$ -s frames, and  $20 \times 60$ -s frames). For [ $^{18}\text{F}$ ]FDG imaging, animals were fasted overnight, injected with approximately 1 mCi of [ $^{18}\text{F}$ ]FDG, and imaged at 1 h after injection. Time-activity curves were generated from regions of interest drawn to encompass the entire tumor.

## RESULTS

We have demonstrated previously that 2-DG treatment of cancer cells causes apoptosis (10). Transformed cells appear to be more sensitive to the effect of 2-DG than their normal counterparts (42). When combined with IR or certain chemotherapeutic agents, 2-DG acts as a sensitizer in causing cancer cell death (42, 43). From these experiments, we predicted that 2-DG would enhance the effect of other tumor-specific therapies.

Fig. 2. Optimal administration of 2-DG as determined by microPET. 2-DG (20 mg) was mixed with [ $^{18}\text{F}$ ]FDG (1 mCi) and administered i.g., i.p., i.v., or s.c. MicroPET imaging was performed at 1 and 3 h after administration. SUV is defined as the ratio of activity in tissue/milliliter to the activity in the injected dose/mouse body weight. *IG*, i.g.; *SC*, s.c.; *IV*, i.v.; *IP*, i.p. Bars, SE.



2-DG has been administered p.o., i.p., and i.v. in several animal tumor models (18, 50, 51). We first determined the optimal method of administering 2-DG using [ $^{18}\text{F}$ ]FDG as a tracer and surrogate for 2-DG. This allowed the use of microPET imaging to examine organ distribution. Although the affinity for enzymes involved in the metabolism of 2-DG and FDG may differ, both FDG and 2-DG enter cells through the glucose transporter and are both phosphorylated by hexokinase (52). 2-DG was mixed with [ $^{18}\text{F}$ ]FDG and administered i.g., i.v., i.p., or s.c. to mice. Distribution of the [ $^{18}\text{F}$ ]FDG was determined at 1 and 3 h after administration. As seen in Fig. 2A, the majority of the [ $^{18}\text{F}$ ]FDG remained in the stomach at 3 h when administered i.g. When 2-DG/[ $^{18}\text{F}$ ]FDG was injected s.c. in the right flank, the majority of the radioactivity was retained in the s.c. tissue over the right kidney at 1 h, and by 3 h most of the [ $^{18}\text{F}$ ]FDG had been absorbed (Fig. 2B). 2-DG/[ $^{18}\text{F}$ ]FDG injected either i.v. or i.p. resulted in a similar distribution between organs and comparable SUVs at 1 and 3 h (Fig. 2, C and D). The majority of the tracer at 1 h was detected in the brain, heart, and kidneys. The SUVs for these organs decreased ~50% by 3 h. These results indicate that [ $^{18}\text{F}$ ]FDG mixed with 2-DG is readily absorbed when given i.p. or i.v. In all subsequent treatment experiments, 2-DG was administered i.p.

We next determined the optimal dose of 2-DG. Previous experiments have reported the LD<sub>50</sub> for 2-DG as 4.5 mg/g of body weight when injected i.p. in mice (25), and in humans doses up to 200 mg/kg i.v. or p.o. have been administered (50, 53). 2-DG was injected i.p. daily at doses from 0.5 mg/g of body weight to 2 mg/g of body weight. Doses up to 2 mg/g of body weight (40 mg) injected i.p. daily resulted in no weight loss, change in appetite, or other constitutional symptoms (Fig. 3A).

To determine the effect of 2-DG on tumor growth and uptake of [ $^{18}\text{F}$ ]FDG, we used the highly aggressive EMT-6 mouse mammary carcinoma cell line as a breast tumor model. This cell line has been well characterized and used extensively to investigate hypoxic agents because EMT-6 solid tumors contain a significant hypoxic fraction dependent on the size of the tumor (54–56). Untreated EMT-6 tumors will double in volume every 4–5 days. 2-DG treatment beginning day 4 after tumor implantation resulted in a mild inhibition of tumor growth (Fig. 3B). For example on day 13, 2-DG given at 40 mg/mouse inhibited tumor growth by ~40%. No systemic toxicity was observed at this dose. Higher doses of 2-DG in non-tumor-bearing mice led to

postinjection lethargy. Overall survival was unchanged at all doses of 2-DG treatment compared with control mice.

EMT-6 tumors established in BALB/c mice selectively accumulate FDG as determined by [ $^{18}\text{F}$ ]FDG microPET imaging (Fig. 4). MicroPET imaging was performed using [ $^{18}\text{F}$ ]FDG on various days after commencing daily treatment with 2-DG to determine whether uptake changed over time of treatment. It has been reported that long-term growth of cells *in vitro* in the presence of 2-DG can result in decreased

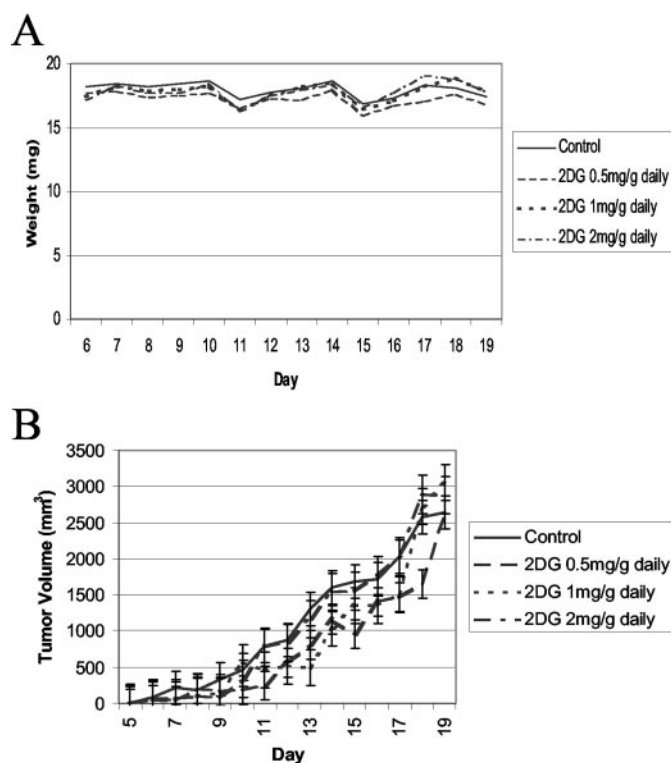


Fig. 3. Dose response of 2-DG administration. EMT-6 tumors were implanted on day zero, and 2-DG at the indicated dose was administered daily i.p. beginning on day 5. Tumor size and animal weights were recorded daily. Each point represents the average tumor volume or weight of five mice. Error bars represent the range of tumor size. A, average weight; B, average tumor volume

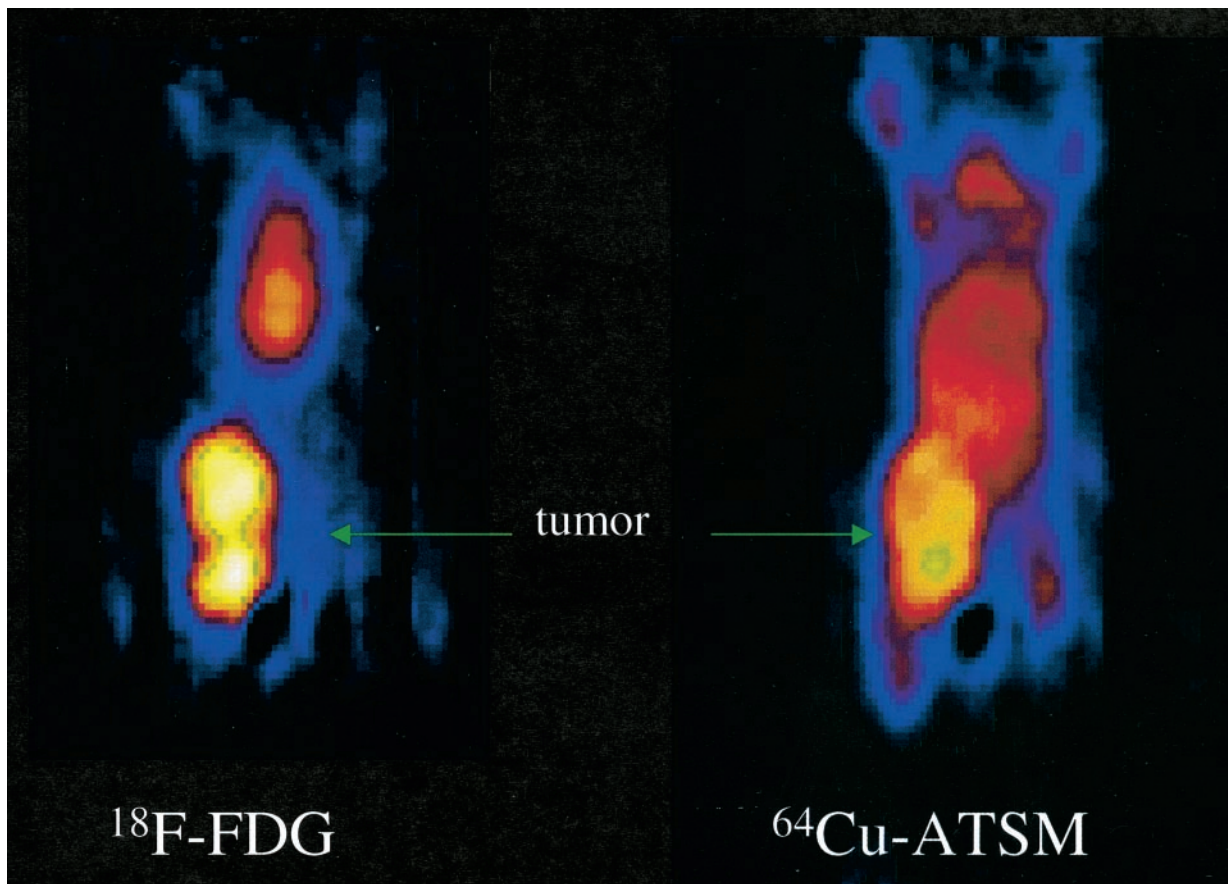


Fig. 4. Coronal microPET images of an EMT-6 tumor-bearing mouse. MicroPET images shown are from the same mouse on day 19 of tumor growth scanned 1 h after injection with [ $^{18}\text{F}$ ]FDG (left panel) and on day 20 of tumor growth 20 min after injection with  $^{64}\text{Cu}$ -ATSM (right panel). This mouse received 2-DG at a dose of 40 mg/kg daily from day 6 of tumor growth.

2-DG-induced toxicity, thought to be related to changes in the transport activity of Glut 1 (57). Mice bearing EMT-6 tumors were treated with 2-DG daily at 40 mg/mouse (2 mg/g) and imaged on days 1, 7, 9, 11, and 14 after the start of treatment. On the day of imaging, 2-DG was coinjected with [ $^{18}\text{F}$ ]FDG in animals undergoing treatment. Brain was used as a control because it has high uptake of [ $^{18}\text{F}$ ]FDG. As seen in Fig. 5A,  $^{18}\text{F}$ -FDG uptake by brain was relatively constant for the duration of the treatment with and without 2-DG treatment. The amount of uptake of [ $^{18}\text{F}$ ]FDG by the brain at all time points was slightly less than half of nontreated animals. Untreated EMT-6 tumors increased the amount of [ $^{18}\text{F}$ ]FDG uptake to day 7, and then this gradually decreased (Fig. 5B, left panel). EMT-6 tumors treated with 2-DG maintained a relatively constant uptake of [ $^{18}\text{F}$ ]FDG throughout the treatment period, which was lower than the amount taken up by nontreated animals (Fig. 5B, right panel). These data indicate that tumor resistance to uptake of [ $^{18}\text{F}$ ]FDG did not develop during the 2 weeks of treatment with 2-DG, although the constant presence of 2-DG may have affected the tumor cell biology because the peak at 7 days was not observed. These data demonstrate that EMT-6 tumors continue to accumulate [ $^{18}\text{F}$ ]FDG throughout the treatment interval with 2-DG. These data would suggest that resistance to 2-DG uptake by tumor cells does not develop during this time interval of treatment.

The effect of 2-DG on tumor uptake of  $^{64}\text{Cu}$ -ATSM and  $^{64}\text{Cu}$ -PTSM was next determined using microPET imaging and by calculating time-activity curves.  $^{64}\text{Cu}$ -ATSM and  $^{64}\text{Cu}$ -PTSM are compounds of low molecular weight and high membrane permeability that differ by a methyl group in the bis(thiosemicarbazone) complex (Fig. 1B). This change causes a marked difference in biological

properties (35).  $^{64}\text{Cu}$ -PTSM rapidly accumulates in tissues with high blood flow and has been used as a flow indicator (58). With bolus injection, it is retained in tissues by first-pass extraction (59). This is in contrast to  $^{64}\text{Cu}$ -ATSM, which has been used to delineate hypoxic tissues (27, 28, 34). *In vivo*,  $^{64}\text{Cu}$ -ATSM is rapidly taken up by all tissues; however, it is washed out of normoxic tissues over time, and the copper remains only in hypoxic cells (28, 33). The difference in properties between  $^{64}\text{Cu}$ -ATSM and  $^{64}\text{Cu}$ -PTSM are thought to be attributable to the redox potentials of the complexes (28). The redox potential of  $^{64}\text{Cu}$ -PTSM is  $-208$  mV, and  $^{64}\text{Cu}$ -ATSM is  $-297$  mV.  $^{64}\text{Cu}$ -PTSM is reduced in normal tissues at the complex I site of the electron transport chain using NADH as the electron donor (60). Under normoxic conditions,  $^{64}\text{Cu}$ -ATSM is reduced less efficiently than  $^{64}\text{Cu}$ -PTSM at the complex I site. It is thought that under hypoxic conditions, depletion of oxygen causes hyperreduction of complex I and an increase in NADH concentration, which is thought to account for the increased retention of  $^{64}\text{Cu}$  from  $^{64}\text{Cu}$ -ATSM in hypoxic tissues (35). Alternatively,  $^{64}\text{Cu}$  retention from  $^{64}\text{Cu}$ -ATSM in cancer cells may be attributable to reduction of the copper by the microsomal fraction of tumor cells rather than by mitochondria-associated enzymes (61). In PET imaging of  $^{64}\text{Cu}$ -ATSM or  $^{64}\text{Cu}$ -PTSM, it is the  $^{64}\text{Cu}$  radioactive decay and its localization that is collated, regardless of the chemical and oxidation state of the copper.

2-DG was administered to mice 1 day before and on the day of the imaging. The brain was used as a control organ for the comparison between  $^{64}\text{Cu}$ -ATSM and  $^{64}\text{Cu}$ -PTSM. As seen in Fig. 6A,  $^{64}\text{Cu}$ -PTSM rapidly crosses the blood-brain barrier and is retained in the brain tissue.  $^{64}\text{Cu}$ -ATSM, although initially extracted efficiently from

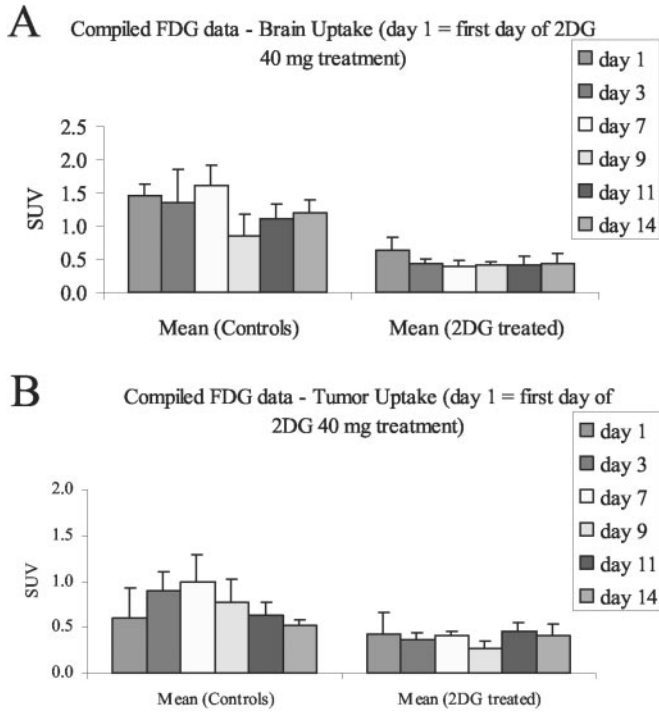


Fig. 5. [ $^{18}\text{F}$ ]FDG uptake by tumor or brain during treatment with 2-DG. EMT-6 tumor-bearing mice were treated with 2-DG (2 mg/g of body weight) beginning 5 days after implantation of tumor cells where indicated. 2-DG was coincjected with [ $^{18}\text{F}$ ]FDG. PET imaging was performed on the indicated dates after the start of treatment. *Right panel*, no 2-DG treatment; *left panel*, 2-DG injected daily. *A*, uptake of [ $^{18}\text{F}$ ]FDG by brain. *B*, uptake of [ $^{18}\text{F}$ ]FDG by EMT-6 tumor. Bars, SD.

the blood pool into the brain, is not reduced intracellularly and is released from the cells (Fig. 6C). The  $^{64}\text{Cu}$ -PTSM values are lower than  $^{64}\text{Cu}$ -ATSM because there has been uptake of  $^{64}\text{Cu}$ -PTSM in other organs before brain delivery, and thus, less activity is available for extraction.  $^{64}\text{Cu}$ -ATSM is released from normoxic tissue, and therefore, more is delivered to the brain. As evidenced by the time-activity curves,  $^{64}\text{Cu}$ -ATSM is subsequently washed out over time. This is consistent with results reported previously (28). EMT-6 tumors demonstrated a rapid uptake and retention of  $^{64}\text{Cu}$ -PTSM, similar to that observed with brain, in both control and 2-DG-treated animals, indicating a high blood flow to the tumor (Fig. 6B). In contrast, when  $^{64}\text{Cu}$ -ATSM was used as the tracer, an increase in uptake and retention within tumor was observed with 2-DG treatment that was not observed in control animals (Fig. 6D). Uptake and retention of  $^{64}\text{Cu}$ -ATSM by EMT-6 tumors was increased up to 5-fold with 40 mg/mouse 2-DG treatment (Fig. 6D), whereas 10 mg/mouse 2-DG caused a 2-fold increased uptake and retention of 2-DG. The 2-DG effect on uptake and retention was only observed for the hypoxia-specific agent  $^{64}\text{Cu}$ -ATSM and not with the nonhypoxia-selective agent  $^{64}\text{Cu}$ -PTSM. These data indicate that 2-DG pretreatment of animals leads to an increased uptake and retention of the hypoxia-specific agent  $^{64}\text{Cu}$ -ATSM by tumors.

Given that 2-DG treatment of EMT-6 tumor-bearing mice leads to the increased accumulation of  $^{64}\text{Cu}$ -ATSM within tumors, we hypothesized that this combined treatment would lead to a higher local dose of radiation therapy, resulting in a more efficient tumor cell killing. This would translate into greater inhibition of tumor growth and improved overall survival of the animals. To test this, EMT-6 tumor-bearing mice were injected with 2-DG daily and given a single dose (2 mCi) of either  $^{64}\text{Cu}$ -ATSM or  $^{64}\text{Cu}$ -PTSM. Combining 2-DG with either  $^{64}\text{Cu}$ -ATSM or  $^{64}\text{Cu}$ -PTSM caused a relative inhibition of tumor growth (Fig. 7). Mice treated with  $^{64}\text{Cu}$ -PTSM plus 2-DG

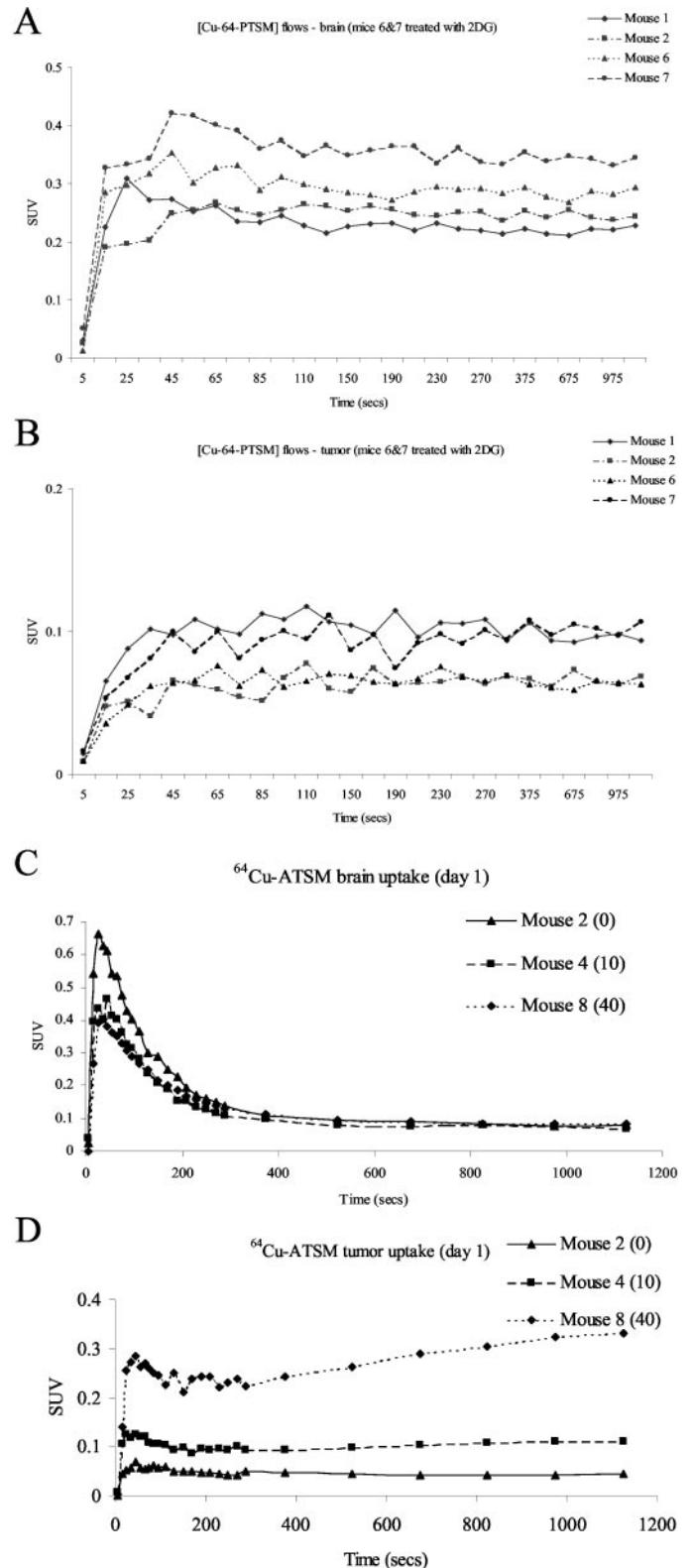


Fig. 6. 2-DG effect on uptake time-activity curves of  $^{64}\text{Cu}$ -ATSM or  $^{64}\text{Cu}$ -PTSM. Note different scales on the y-axes. Animals received injections of 2-DG 4 and 24 h before the injection of  $^{64}\text{Cu}$ -ATSM or  $^{64}\text{Cu}$ -PTSM. Time-activity curves were generated by drawing regions of interest over EMT-6 tumors or mouse brains and calculating SUVs. Data are normalized to the amount of radioactivity injected. For *A* and *B*, mouse 1 and mouse 2 received no treatment, mouse 6 was injected with 10 mg of 2-DG, and mouse 7 was injected with 40 mg of 2-DG. For *C* and *D*, numbers in parentheses indicate the amount of 2-DG injected in mg/mouse. *A*, mouse brain with  $^{64}\text{Cu}$ -PTSM. *B*, EMT-6 tumor with  $^{64}\text{Cu}$ -PTSM. *C*, mouse brain with  $^{64}\text{Cu}$ -ATSM. *D*, EMT-6 tumor with  $^{64}\text{Cu}$ -ATSM.

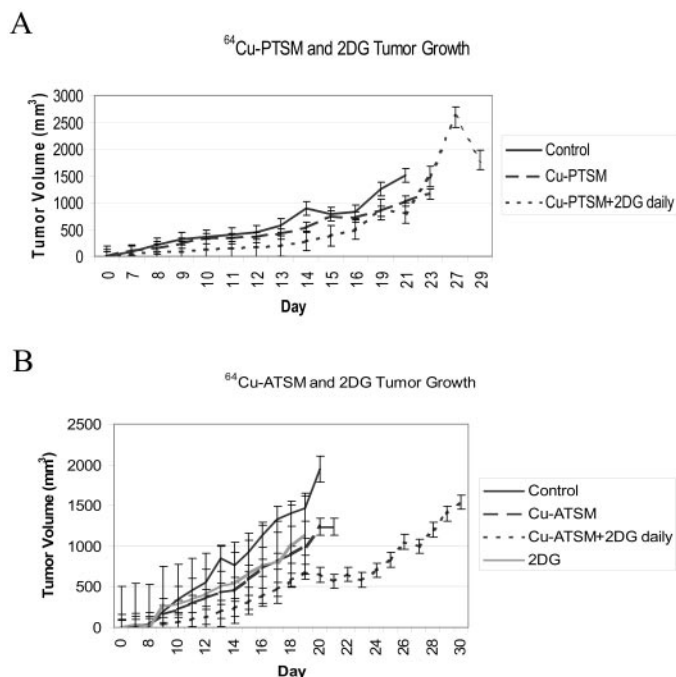


Fig. 7. Effect of 2-DG on tumor growth after treatment with  $^{64}\text{Cu}$ -ATSM or  $^{64}\text{Cu}$ -PTSM. EMT-6 tumors were implanted on day zero. Mice received daily i.p. injections with 2-DG (40 mg/mouse) beginning on day 4. A single dose (2 mCi/mouse) of either  $^{64}\text{Cu}$ -PTSM (A) or  $^{64}\text{Cu}$ -ATSM (B) was injected i.v. on day 5 where indicated. Tumor size and animal weights were recorded daily. Mice were sacrificed if the tumor ulcerated or was  $>10\%$  of body weight. Each point represents the average tumor volume or weight of five mice except for the treatment groups  $^{64}\text{Cu}$ -PTSM alone and with 2-DG. These two groups contained four mice only because of the nongrowth of tumors in two mice. Error bars represent the range of tumor size. A, mice treated with  $^{64}\text{Cu}$ -PTSM with or without 2-DG. B, mice treated with  $^{64}\text{Cu}$ -ATSM with or without 2-DG.

demonstrated an initial inhibition of tumor growth up to day 14 (Fig. 7A). However, after this time the tumors grew at the same rate as controls. No significant difference in overall survival was observed between the  $^{64}\text{Cu}$ -PTSM plus 2-DG and the other treatments ( $P = 0.29$ ; Fig. 8A). Mice treated with  $^{64}\text{Cu}$ -ATSM and 2-DG also demonstrated an inhibition of tumor growth (Fig. 7B). The greatest inhibition of tumor growth occurred with the combined treatment of  $^{64}\text{Cu}$ -ATSM and daily 2-DG (Fig. 7B). For example, on day 17, tumors treated with 2-DG and  $^{64}\text{Cu}$ -ATSM were 3-fold smaller than control animals and approximately half the size of tumor with each treatment alone. Furthermore, in animals treated with a single dose of 2 mCi of  $^{64}\text{Cu}$ -ATSM and 40 mg of 2-DG daily, 50% survival was  $\sim 29$  days compared with 17 days for control animals and 2-DG alone-treated animals and 20 days for  $^{64}\text{Cu}$ -ATSM-treated animals (Fig. 8B). Twenty-two days after treatment, 40% of mice treated with 2-DG and  $^{64}\text{Cu}$ -ATSM were alive. In contrast, 100% of mice treated with saline had to be killed by 22 days because the tumors had grown  $>2$  g or had ulcerated through the skin. Calculation of significance using the log-rank test gives a  $P$  of 0.011 for the comparison involving  $^{64}\text{Cu}$ -ATSM plus 2-DG and other treatments, indicating statistically significant differences between the groups. We watched for weight loss and lethargy, and no significant toxicity was observed. This set of experiments indicates that 2-DG combined with  $^{64}\text{Cu}$ -ATSM inhibits tumor growth more than each agent alone and significantly increases overall survival with minimal effect on the host animal.

The  $t_{1/2}$  of  $^{64}\text{Cu}$  is 12 h, and  $^{64}\text{Cu}$  is completely decayed by 5 days. To determine whether 2-DG needed to be present during the peak activity of  $^{64}\text{Cu}$  or the lifetime of the mouse, 2-DG was given for a total of 6 days (1 day before treatment and 5 days after treatment with  $^{64}\text{Cu}$ -ATSM). As seen in Fig. 8B, there was no change in survival

when 2-DG was administered for 5 days compared with controls. The maximal effect was observed when 2-DG was present for the lifetime of the mouse.

## DISCUSSION

Alterations in the activity of processes that affect cellular metabolism may affect the sensitivity of cancer cells to other therapies. This has been the basis of combination chemotherapy and radiation therapies. We have shown previously that 2-DG-induced metabolic alterations cause apoptosis of cancer cells and significantly potentiate the cytotoxic effects of ionizing radiation in human cancer cell lines (10, 42). In the present study, we demonstrate that treatment with 2-DG potentiates the cytotoxic effect of targeted radiation therapy with  $^{64}\text{Cu}$ -ATSM in a mouse tumor model of aggressive breast cancer.

The efficacy of conventional radiotherapy is limited by the presence of a hypoxic, radioresistant, and repair-proficient subset of tumor cells. This has led to the development and testing of radiosensitizers. Previously tested radiosensitizers have been limited by their clinical toxicity and lack of clinical effectiveness (1, 3). In the present study, we have used a hypoxic tumor model to demonstrate that 2-DG acts as a radiosensitizer for  $^{64}\text{Cu}$ -ATSM.  $^{64}\text{Cu}$ -ATSM is selectively retained in hypoxic cells *in vitro* and tumor cells *in vivo* (28) and has been used for targeted radiotherapy in animal models of tumors and tumor metastases (28, 34). In patients with cervical carcinoma, accu-

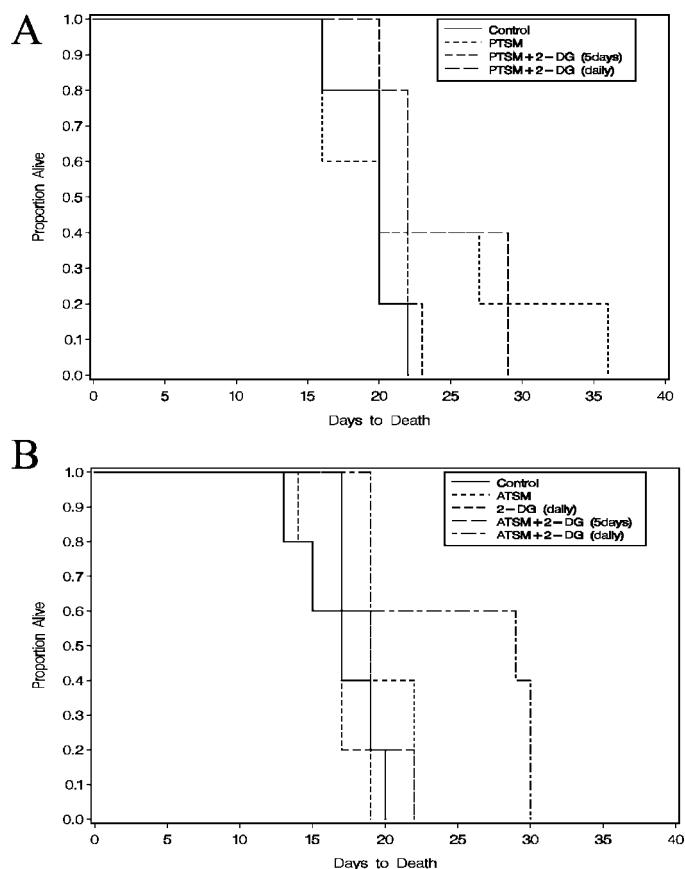


Fig. 8. Effect of 2-DG on survival after treatment with  $^{64}\text{Cu}$ -ATSM or  $^{64}\text{Cu}$ -PTSM. Estimated survival distribution function was generated using a Kaplan-Meier time-to-death analysis. For comparison involving treatments with  $^{64}\text{Cu}$ -PTSM treatments with or without 2-DG, the log-rank test gives a  $P$  of 0.29, indicating that there are no significant differences between groups (A). The  $^{64}\text{Cu}$ -ATSM treatments with or without 2-DG comparison has a  $P$  of 0.011 from the same test, indicating that there are statistically significant differences between the groups (B).

mulation of  $^{64}\text{Cu}$ -ATSM correlated with tumor hypoxia and poor patient outcome (30).

Copper radioisotopes have been studied extensively for therapeutic use (62, 63).  $^{64}\text{Cu}$  has been identified as an attractive radionuclide for therapy because it decays with a number of therapeutic emissions, has a short half-life (12.7 h), is a natural constituent of DNA, and functions as a copper cation in cells (63). Furthermore,  $^{64}\text{Cu}$  decays with  $\beta^+$  emissions, which allows for simultaneous imaging by PET (64, 65). The radiobiological effect of  $^{64}\text{Cu}$  is complex because of the multiple types of emissions, and cell kill may depend on the intracellular distribution of the radionuclide. Previous studies have shown that  $^{64}\text{Cu}$  is cytotoxic, as shown by a linear cell survival curve when plotted on a logarithmic scale (62, 63). This is an interesting result, considering that  $^{64}\text{Cu}$  is considered a low LET nuclide, and the survival curves of low LET nuclides generally have a large shoulder. Low LET decay is characteristic of  $\beta$ -emitters, and high LET decay is characteristic of nuclides that decay by particles or Auger electrons (66–68). With radionuclides such as  $^{64}\text{Cu}$ , which have both  $\beta$  and Auger emissions, the copper ion needs to be incorporated in the cell nucleus for the Auger electrons to cause cell kill because of the short path length of emitted particles. This is in contrast to the  $\beta$  emission, which can result in a “cross-fire” energy from neighboring cells. Because copper has an important role in the function of the cell nucleus, playing a structural role in nuclear matrix proteins, copper trafficking to the cell nucleus may partially explain the behavior of  $^{64}\text{Cu}$  as a high LET emitter. If the copper radionuclide were in the vicinity of the DNA upon decay, the daughter species could collide (“recoil”) with the DNA, causing irreparable damage and cell death. Multiple factors require consideration to understand the relative biological effectiveness of the emitted radiations of  $^{64}\text{Cu}$ , including the time-dose pattern, the distribution of the radionuclide in the target tissue within the cell, and the absorbed dose/energy. Unfortunately, little data are available concerning the influence of this latter factor. It is clear that there is an increasing need to understand the complexities of the dose rate in radiotherapy studies, which would allow a more exacting determination of biological response to radiotherapy.

High glucose transporter levels have been found in areas of tumor hypoxia and in cancer cells that are resistant to cytotoxic drugs and ionizing radiation (17, 20, 69). It has been suggested that high glucose transporter expression is a survival response of cancer cells that allows growth in poor nutrient conditions and counteracts apoptotic signals in cancer cells (8, 9). 2-DG accumulates in cells by facilitated diffusion through the glucose transporter (11, 70). Because of intrinsic metabolic alterations in cancer cells, 2-DG becomes selectively trapped within cancer cells (14). Furthermore, hypoxic conditions lead to an increase in 2-DG uptake *in vitro* (17, 69, 71). These data suggest that 2-DG localizes to cancer cells, which may be particularly resistant to chemotherapy or radiation therapy.

Daily injections of 2-DG do not appear to alter the uptake of [ $^{18}\text{F}$ ]FDG accumulation at various times after initiation of treatment. This indicates that tumors do not become resistant to 2-DG uptake over time, as has been reported in tissue culture (57). Untreated EMT-6 tumors gradually increase [ $^{18}\text{F}$ ]FDG uptake to a peak at 7 days. This may reflect the evolving biology of tumor growth, which leads to increasing hypoxia followed by angiogenesis (1) or a change in the mass of viable cells. We have reported previously that 2-DG treatment of breast cancer cells *in vitro* results in an increased expression of glucose transporter and an increase in glucose uptake (10). It is possible that a similar phenomenon occurs in solid tumors. Tumor cells may adapt to the presence of 2-DG by altering transporter levels such that they can maintain an adequate level of glucose uptake because there may be a limited ability to adapt to other forms of energy metabolism.

Pretreatment with 2-DG results in increased uptake and retention of  $^{64}\text{Cu}$ -ATSM by EMT-6 mouse breast cancer tumors. *In vitro*, treatment with 2-DG causes rapid generation of reactive oxygen species and alterations in intracellular thiol levels (23, 24, 42). These intracellular alterations may account for the increased accumulation of  $^{64}\text{Cu}$ -ATSM within the breast cancer tumors after 2-DG treatment. The observed increased accumulation of  $^{64}\text{Cu}$ -ATSM may be a result of greater uptake by each individual tumor cell or by uptake by a greater percentage of cells. Experiments comparing the distribution of [ $^{18}\text{F}$ ]FDG and  $^{64}\text{Cu}$ -ATSM in solid tumors revealed regions of  $^{64}\text{Cu}$ -ATSM uptake that were distinctly different from regions of increased uptake of  $^{18}\text{F}$ FDG, indicating that [ $^{18}\text{F}$ ]FDG and  $^{64}\text{Cu}$ -ATSM localize to different regions of the tumor (33). In the tumor microenvironment, cells in close proximity to the vasculature would presumably have higher [ $^{18}\text{F}$ ]FDG uptake compared with cells remote from the vascular bed, despite the higher glucose transporter levels found in hypoxic tissue attributable to the increased availability. It is therefore tempting to speculate that those tumor cells with high [ $^{18}\text{F}$ ]FDG uptake that are not hypoxic or are chronically hypoxic may be altered metabolically by 2-DG such that  $^{64}\text{Cu}$ -ATSM accumulates in these cells. This may result in a more homogeneous distribution of  $^{64}\text{Cu}$ -ATSM within the tumor, which could result in a greater tumor cell kill. Toxic Auger particles have a mean range of penetrating radiation only in the nanometer range (40), more cells would be affected, and the contribution of cross-fire to cell kill from the  $\beta^-$  emission would increase. Maximal tumoricidal effect would therefore be anticipated with a more uniform distribution of  $^{64}\text{Cu}$  throughout the tumor. Alternatively, the administration of 2-DG may result in an increase in uptake of  $^{64}\text{Cu}$ -ATSM into the hypoxic regions. Consequently, the Auger emission would be even more effective within the hypoxic region before addition of the radiosensitizer. After the addition of the radiosensitizer, all of the longer ranged  $\beta^-$  emissions could be providing the enhanced therapy to the normoxic areas of the tumor. The mechanism underlying the effect of 2-DG on  $^{64}\text{Cu}$ -ATSM accumulation is currently under investigation in our laboratories.

The maximal effect of 2-DG was observed when the therapy was administered for the duration of the animal's life. *In vivo* studies in animal tumors have shown that administration of 2-DG just before irradiation results in a significant delay in tumor growth, leading to an improvement in survival of animals (43). Although 2-DG alone causes cancer cells to undergo apoptosis *in vitro* (10, 23), it is likely that the effects of 2-DG in enhancing radiation sensitivity are multifactorial and include effects on the metabolic state of the cell, resulting in a depletion of radioprotective sulfhydryl groups (42) and depletion of ATP, which in turn results in the inability of the cell to repair radiation-induced damage (72). A substantial body of data suggests that DNA is the target of the cytotoxic effects of radiation (73). Double-strand DNA breaks are responsible for radiation-induced cellular death, and differences in cellular sensitivity to radiation may reflect the ability of the cell to repair this damage. 2-DG treatment through depletion of intracellular energy may impair the ability of the cell to repair double-stranded DNA breaks, and as a consequence, the number of lethal lesions increases (74). Gene activation, transcription, and protein synthesis in response to radiation damage are required for the cell to survive a dose of radiation. These cellular processes leading to error-free repair require continuous metabolic energy, which is frequently supplied by enhanced glycolysis. The presence of 2-DG for several hours after radiation has been reported to selectively inhibit the postirradiation repair processes in cells, thereby enhancing radiation damage (75). Finally, 2-DG by changing the metabolic state of the cell may lead to depletion in the cell of radioprotective thiols, which may act as free radical scavengers (42).

For targeted therapy to be useful, there must be greater delivery of

the cytotoxic agent to tumor cells than to normal cells (76). In these experiments, we have used 2-DG to enhance the cytotoxic effect of <sup>64</sup>Cu-ATSM. Each of these agents is selectively accumulated to higher concentration in tumors compared with normal tissues as a result of physiological differences between tumors and normal cells. In general, using two cancer cell-selective agents should increase the toxicity to cancer cells while minimizing damage to normal tissue. Furthermore, disseminated tumors cannot be targeted with conventional radiation. Biologically targeted radiotherapy with agents such as <sup>64</sup>Cu-ATSM are designed to overcome this constraint and would theoretically allow treatment of metastatic disease (76). A limitation of targeted radiotherapy has been the heterogeneity of radionuclide uptake on a cell-to-cell basis and within a tumor, which may limit clinical effectiveness of these forms of treatment. One approach to overcome this limitation may be to use a combination of tumor-specific cytotoxic agents or radiosensitizers.

The results of this study are of potential clinical interest and may provide a rationale for combining agents such as 2-DG and <sup>64</sup>Cu-ATSM in the treatment of relatively hypoxic human tumors with high glucose uptake. Pretreatment imaging with [<sup>18</sup>F]FDG and <sup>64</sup>Cu-ATSM would allow stratification of tumor phenotypes such that those tumors that are most susceptible would be selected for treatment. Although <sup>64</sup>Cu-ATSM has not yet been tested as a therapeutic agent in human studies, the absorbed dose estimates for <sup>64</sup>Cu-ATSM have been calculated by extrapolation from a hamster model (32). In this report, an estimated dose of 7500 mCi of <sup>64</sup>Cu-ATSM for clinical therapy trials in humans would be possible. Absorbed doses are currently being calculated at Washington University in humans using <sup>60</sup>Cu-ATSM and PET in conjunction with the recently reported papers on <sup>60</sup>Cu-ATSM in cervical and non-small cell lung cancer patients (30, 31). 2-DG at doses up to 200 mg/kg has been used in Phase I trials (53). It is possible that clinically effective therapeutic levels may be achievable using this combination of drugs rather than each individually. This type of combination may provide a unique treatment for chemotherapy-refractory tumors as well as disseminated disease. Although the current studies focus on breast cancer, hypoxia and increased glucose transport are observed in a wide variety of primary solid tumors and metastatic disease. We think that combinations such as 2-DG and <sup>64</sup>Cu-ATSM will result in an effective, selective treatment for solid tumors and provide a new therapy for control of local and distant disease.

## ACKNOWLEDGMENTS

We thank Vainey Jain for helpful discussions, Dr. Deborah McCarthy and Todd Perkins for the production of <sup>64</sup>Cu, and Kim Trinkaus for statistical calculations. We also thank the Small Animal Imaging Core of the Alvin J. Siteman Cancer Center at Washington University and Barnes-Jewish Hospital in St. Louis, Missouri for additional support of the microPET imaging and the Statistics Core for statistical analysis.

## REFERENCES

- Brown, M. The hypoxic cell: a target for selective cancer therapy. Eighteenth Bruce F. Cain Memorial Lecture. *Cancer Res.*, 59: 5863–5870, 1999.
- Ryan, P., and Chabner, B. On receptor inhibitors and chemotherapy. *Clin. Cancer Res.*, 6: 4607–4609, 2000.
- Coleman, C., and Mitchell, J. Clinical radiosensitization: why it does and does not work. *J. Clin. Oncol.*, 17: 1–3, 1999.
- Hortobagyi, G., and Budzar, A. Current status of adjuvant chemotherapy for primary breast cancer: progress and controversy. *CA Cancer J. Clin.*, 45: 199–226, 1995.
- Tannock, I. Treatment of cancer with radiation and drugs. *J. Clin. Oncol.*, 14: 3156–3174, 1996.
- Warburg, O. On the origin of cancer cells. *Science (Wash. DC)*, 123: 309–314, 1956.
- Weber, G. Enzymology of cancer cells. *N. Engl. J. Med.*, 296: 541–551, 1977.
- Kan, O., Baldwin, S., and Whetton, A. Apoptosis is regulated by the rate of glucose transport in an interleukin 3 dependent cell line. *J. Exp. Med.*, 180: 917–923, 1994.
- Vander Heiden, M., Plas, D., Rathmell, J., Fox, C., Harris, M., and Thompson, C. Growth factors can influence cell growth and survival through effects on glucose metabolism. *Mol. Cell. Biol.*, 21: 5899–5912, 2001.
- Aft, R., Zhang, F., and Gius, D. Evaluation of 2-deoxy-D-glucose as a chemotherapeutic agent: mechanism of cell death. *Br. J. Cancer*, 87: 805–812, 2002.
- Waki, A., Kato, H., Yano, R., Sadato, N., Yokoyama, A., Ishii, Y., Yonekura, Y., and Fujibayashi, Y. The importance of glucose transport activity as the rate-limiting step of 2-deoxyglucose uptake in tumor cells *in vitro*. *Nucl. Med. Biol.*, 25: 593–597, 1998.
- Younes, M., Lechago, L., Somoano, J., Mosharaf, M., and Lechago, J. Wide distribution of the human erythrocyte glucose transporter Glut1 in human cancers. *Cancer Res.*, 56: 1164–1167, 1996.
- Brown, R., and Wahl, R. Over-expression of Glut1 glucose transporter in human breast cancer: an immunohistochemistry study. *Cancer (Phila.)*, 15: 2979–2985, 1993.
- Gallagher, B., Fowler, J., Gutterson, N., MacGregor, R., Wan, C., and Wolf, A. Metabolic trapping as a principle of radiopharmaceutical design: some factors responsible for the biodistribution of [<sup>18</sup>F]2-deoxy-2-fluoro-D-glucose. *J. Nucl. Med.*, 19: 1154–1161, 1978.
- Arora, K., Parry, D., and Pedersen, P. Hexokinase receptors: preferential enzyme binding in normal cells to non-mitochondrial sites and in transformed cells to mitochondrial sites. *J. Bioenerg. Biomembr.*, 24: 47–53, 1992.
- Rempel, A., Mathupala, S., Griffin, C., Hawkins, A., and Pedersen, P. Glucose catabolism in cancer cells: amplification of the gene encoding type II hexokinase. *Cancer Res.*, 56: 2468–2471, 1996.
- Bos, R., van der Hoeven, J., van der Wall, E., van der Groep, P., van Diest, P., Comans, E., Joshi, U., Semenza, G., Lammertsma, A., and Moolthoff, C. Biological correlates of 18Fluorodeoxyglucose uptake in human breast cancer measured by positron emission tomography. *J. Clin. Oncol.*, 20: 379–388, 2002.
- Kern, K., and Norton, J. Inhibition of established rat fibrosarcoma growth by the glucose antagonist 2-deoxy-D-glucose. *Surgery*, 102: 380–385, 1987.
- Liu, X., Kim, C., Kurbanov, F., Honzatkó, R., and Fromm, H. Dual mechanisms for glucose 6-phosphate inhibition of human brain hexokinase. *J. Biol. Chem.*, 274: 31155–31159, 1999.
- Nelson, C., Wang, J., Leav, I., and Crane, P. The interaction among glucose transport, hexokinase, and glucose-6-phosphatase with respect to <sup>3</sup>H-2-deoxyglucose in murine tumor models. *Nucl. Med. Biol.*, 23: 533–541, 1996.
- Liu, X., Gupta, A., Corry, P., and Lee, Y. Hypoglycemia-induced c-Jun phosphorylation is mediated by c-Jun N-terminal kinase 1 and Lyn kinase in drug-resistant human breast carcinoma MCF-7/ADR cells. *J. Biol. Chem.*, 272: 11690–11693, 1997.
- Spitz, D., Sim, J., Ridnour, L., Galoforo, S., and Lee, Y. Glucose deprivation-induced oxidative stress in human tumor cells: a fundamental defect in metabolism? *Ann. NY Acad. Sci.*, 899: 349–362, 2000.
- Nomura, K., Imai, H., Koumura, T., Arai, M., and Nakagawa, Y. Mitochondrial phospholipid hydroperoxide glutathione peroxidase suppresses apoptosis mediated by a mitochondrial death pathway. *J. Biol. Chem.*, 274: 29294–29302, 1999.
- Kaplan, O., Lyon, R., Faustino, P., Straka, E., and Cohen, J. Effects of 2-deoxyglucose on drug-sensitive and drug-resistant human breast cancer cells: toxicity and magnetic resonance spectroscopy of metabolism. *Cancer Res.*, 50: 544–551, 1990.
- Laszlo, J., Humphreys, S., and Goldin, A. Effects of glucose analogues (2-deoxy-D-glucose, 2-deoxy-D-galactose) on experimental tumors. *J. Natl. Cancer Inst.*, 24: 267–280, 1960.
- Mohanti, B., Rath, G., Anantha, N., Kannan, V., Das, B., Chandramouli, B., Banerjee, A., Das, S., Jena, A., Ravichandran, R., Shai, U. P., Kumar, R., Kapoor, N., Kalia, V., Dwarkanath, B. S., and Jain, V. Improving cancer radiation therapy with 2-deoxy-D-glucose: Phase I/II clinical trials on human cerebral gliomas. *Int. J. Radiat. Oncol. Biol. Phys.*, 35: 103–111, 1996.
- Fujibayashi, Y., Taniuchi, H., Yonekura, Y., Ohtani, H., Konishi, J., and Yokoyama, A. Copper-62-ATSM: a new hypoxia imaging agent with high membrane permeability and low redox potential. *J. Nucl. Med.*, 38: 1155–1160, 1997.
- Lewis, J., McCarthy, D., McCarthy, T., Fujibayashi, Y., and Welch, M. Evaluation of <sup>64</sup>Cu-ATSM *in vitro* and *in vivo* in a hypoxic tumor model. *J. Nucl. Med.*, 40: 177–183, 1999.
- Takahashi, N., Fujibayashi, Y., Yonekura, Y., Welch, M., Waki, A., Tsuchida, T., Sadato, N., Sugimoto, K., and Itoh, H. Evaluation of <sup>62</sup>Cu labeled diacetyl-bis(<sup>N</sup><sup>4</sup>-methylthiosemicarbazone) as a hypoxic tracer in patients with lung cancer. *Ann. Nucl. Med.*, 14: 323–328, 2000.
- Dehdashti, F., Grigsby, P., Mintun, M., Lewis, J., Siegel, B., and Welch, M. Assessing tumor hypoxia in cervical cancer by positron emission tomography with <sup>60</sup>Cu-ATSM: relationship to therapeutic response—a preliminary report. *Int. J. Rad. Onc. Biol. Phys.*, 55: 1233–1238, 2003.
- Dehdashti, F., Mintun, M., Lewis, J., Bradley, J., Govindan, R., Laforest, R., Welch, M., and Siegel, B. *In vivo* assessment of tumor hypoxia in lung cancer with <sup>60</sup>Cu-ATSM. *Eur. J. Nucl. Med.*, 30: 844–850, 2003.
- Lewis, J., Laforest, R., Buettner, T., Song, S., Fujibayashi, Y., Connett, J., and Welch, M. Copper-64-diacetyl-bis(<sup>N</sup><sup>4</sup>-methylthiosemicarbazone): an agent for radiotherapy. *Proc. Natl. Acad. Sci. USA*, 98: 1206–1211, 2001.
- Lewis, J., Sharp, T., Laforest, R., Fujibayashi, Y., and Welch, M. Tumor uptake of copper-diacetyl-bis(<sup>N</sup><sup>4</sup>-methylthiosemicarbazone): effect of changes in tissue oxygenation. *J. Nucl. Med.*, 42: 655–661, 2001.
- Dearling, J., Lewis, J., Mullen, G., Welch, M., and Blower, P. Design of hypoxia-targeting radiopharmaceuticals: selective uptake of copper-64 complexes in hypoxic cells *in vitro*. *Eur. J. Nucl. Med.*, 25: 788–792, 1998.



35. Maurer, R., Blower, P., Dilworth, J., Reynolds, C., Zheng, Y., and Mullen, G. Studies on the mechanism of hypoxic selectivity in copper bis(thiosemicarbazone) radio-pharmaceuticals. *J. Med. Chem.*, *45*: 1420–1431, 2002.
36. Lewis, J., Connet, J., Garbow, J., Buettner, T., Fujibayashi, Y., Fleshman, J., and Welch, M. Copper-64-pyruvaldehyde-bis(*N*<sup>4</sup>-methylthiosemicarbazone) for the prevention of tumor growth at wound sites following laparoscopic surgery: monitoring therapy response with microPET and magnetic resonance imaging. *Cancer Res.*, *62*: 445–449, 2002.
37. Connet, J., Anderson, C., Guo, L., Schwarz, S., Zinn, K., Rogers, B., Seigel, B., Philpott, G., and Welch, M. Radioimmunotherapy with a <sup>64</sup>Cu-labeled monoclonal antibody: a comparison with <sup>67</sup>Cu. *Proc. Natl. Acad. Sci. USA*, *93*: 6814–6818, 1996.
38. Lewis, J., Lewis, M., Cutler, P., Srinivasan, A., Schmidt, M., Schwarz, S., Morris, M., Miller, J., and Anderson, C. Radiotherapy and dosimetry of <sup>64</sup>Cu-TETA-Tyr3-octreotate in a somatostatin receptor positive tumor-bearing rat model. *Clin. Cancer Res.*, *5*: 3608–3616, 1999.
39. Adelstein, S. J. The Auger process: a therapeutic promise? *Am. J. Roentgenol.*, *160*: 707–713, 1993.
40. O'Donoghue, J., and Wheldon, T. Targeted radiotherapy using Auger electron emitters. *Phys. Med. Biol.*, *41*: 173–1992, 1996.
41. Hockel, M., and Vaupel, P. Tumor hypoxia: definitions and current clinical, biological, and molecular aspects. *J. Natl. Cancer Inst.*, *93*: 266–276, 2001.
42. Lin, X., Zhang, F., Bradbury, M., Kaushal, A., Spitz, D., Aft, R., and Gius, D. 2-Deoxy-D-glucose induced cytotoxicity and radiosensitization in tumor cells is mediated via disruptions in thiol metabolism. *Cancer Res.*, *63*: 2413–2417, 2003.
43. Purohit, S., and Pohlit, W. Experimental evaluation of the glucose anti-metabolite, 2-deoxy-D-glucose as a possible adjuvant to radiotherapy of tumors. I. Kinetics of growth and survival of Ehrlich ascites cells *in vitro* and of growth of solid tumors after 2-DG and x-irradiation. *Int. J. Radiat. Oncol. Biol. Phys.*, *8*: 495–499, 1981.
44. McCarthy, D., Bass, L., Cutler, P., Shefer, R., Klinkowstein, R., Herrero, P., Lewis, J., Cutler, C., Anderson, C., and Welch, M. High purity production and potential applications of copper-60 and copper-61. *Nucl. Med. Biol.*, *26*: 351–358, 1999.
45. McCarthy, D., Shefer, R., Klinkowstein, R., Bass, L., Margeneau, W., Cutler, C., Anderson, C., and Welch, M. Efficient production of high specific activity <sup>64</sup>Cu using a biomedical cyclotron. *Nucl. Med. Biol.*, *24*: 35–43, 1997.
46. Young, H., Carnochan, P., Zweit, J., Babich, J., Cherry, S., and Ott, R. Evaluation of copper(II)-pyruvaldehyde bis(*N*<sup>4</sup>-methylthiosemicarbazone) for tissue blood flow measurement using a trapped tracer model. *J. Nucl. Med.*, *21*: 336–341, 1994.
47. Hamacher, K., Coenen, H., and Stocklin, G. Efficient stereospecific synthesis of no-carrier-added 2-[<sup>18</sup>F]fluoro-2-deoxy-D-glucose using an aminopolyether supported nucleophilic substitution. *J. Nucl. Med.*, *27*: 235–238, 1986.
48. Cherry, S., Shao, Y., Silverman, R., Meadors, K., Siegel, S., Chatziioannou, A., Young, J., Jones, W., Moyers, J., Newport, D., Boutenouchet, A., Faquhar, T., Andreaco, M., Paulus, M., Binkley, D., Nutt, R., and Phelps, M. MicroPET: a high resolution PET scanner for imaging small animals. *IEEE Trans. Nucl. Sci.*, *44*: 1161–1166, 1997.
49. Defrise, M., Kinahan, D., Townsend, C., Michel, M., and Newport, D. Exact and approximate rebinning algorithms for 3-D PET data. *IEEE Trans. Med. Imaging*, *16*: 145–158, 1997.
50. Landau, B., Laszlo, J., Stengle, J., and Burk, D. Certain metabolic and pharmacologic effects in cancer patients given an infusion of 2-deoxy-D-glucose. *J. Natl. Cancer Inst.*, *21*: 485–494, 1958.
51. Ball, H., Wick, A., and Sanders, C. Influence of glucose anti-metabolites on the Walker tumor. *Cancer Res.*, *17*: 235–239, 1957.
52. Pauwels, E., Strum, E., Bombardieri, E., Cleton, F., and Stokkel, M. Positron-emission tomography with [<sup>18</sup>F]fluorodeoxyglucose. Part I. Biochemical uptake mechanism and its implications for clinical studies. *J. Cancer Res. Clin. Oncol.*, *126*: 549–559, 2000.
53. Mohanti, B., Rath, G., Anantha, N., Kannan, V., Das, B., Chandramouli, B., Banerjee, A., Das, S., Jena, A., Ravichandran, R., Sahi, U., Kumar, R., Kalia, V., Dwarkanath, B., and Jain, V. Improving cancer radiotherapy with 2-deoxy-D-glucose: Phase III trials on cerebral gliomas. *Int. J. Radiat. Oncol. Biol. Phys.*, *35*: 103–111, 1996.
54. Shibamoto, Y., Nishimoto, S., Mi, F., Sasai, K., Kagiya, T., and Abe, M. Evaluation of various types of new hypoxic cell sensitizers using the EMT6 single cell-spheroid-solid tumor system. *Int. J. Radiat. Biol.*, *52*: 347–357, 1987.
55. Franko, A. Hypoxic fraction and binding of misonidazole in EMT6/Ed multicellular tumor spheroids. *Radiat. Res.*, *103*: 89–97, 1985.
56. Moulder, J., and Rockwell, S. Hypoxic fraction of solid tumors: experimental techniques, methods of analysis, and a survey of existing data. *Int. J. Radiat. Oncol. Biol. Phys.*, *10*: 695–712, 1984.
57. Mesmer, O., Lu, Z., and Lo, T. Effects of 2-deoxy-D-glucose on the functional state of the rat myoblast GLUT 1 transporter. *Biochem. Mol. Biol. Int.*, *40*: 217–233, 1996.
58. Herrero, P., Markham, J., Weinheimer, C., Anderson, C., Welch, M., Green, M., and Bergmann, S. Quantification of regional myocardial perfusion with generator-produced <sup>62</sup>Cu-PTSM and positron emission tomography. *Circulation*, *87*: 173–183, 1993.
59. Green, M., Mathias, C., Welch, M., McGuire, A., Perry, D., Fernandez-Rubio, F., Perlmutter, J., Raichle, M., and Bergmann, S. Copper-62-labeled pyruvaldehyde bis(*N*<sup>4</sup>-methylthiosemicarbazone)copper(II): synthesis and evaluation as a possible emission tomography tracer for cerebral and myocardial perfusion. *J. Nucl. Med.*, *31*: 1989–1996, 1990.
60. Shibuya, K., Fujibayashi, Y., Yoshimi, E., Sasai, K., Hiraoka, M., and Welch, M. Cytosolic/microsomal redox pathway: a reductive mechanism of a PET-oncology tracer, Cu-pyruvaldehyde-bis(*N*<sup>4</sup>-methylthiosemicarbazone) (Cu-PTSM). *Ann. Nucl. Med.*, *13*: 287–292, 1999.
61. Obata, A., Yoshimi, E., Waki, A., Lewis, J., Oyama, N., Welch, M., Saji, H., Yonekura, Y., and Fujibayashi, Y. Retention mechanism of hypoxia selective nuclear imaging/radiotherapeutic agent Cu-diacetyl-bis(*N*<sup>4</sup>-methylthiosemicarbazone) (Cu-ATSM) in tumor cells. *Ann. Nucl. Med.*, *15*: 499–504, 2001.
62. Apelgot, S., Coppey, J., Gaudenemer, A., Grisvard, J., Guille, E., Sasaki, I., and Sissoeff, I. Similar lethal effect in mammalian cells for two radioisotopes of copper with different decay schemes, <sup>64</sup>Cu and <sup>67</sup>Cu. *Int. J. Radiat. Biol.*, *55*: 365–384, 1989.
63. Apelgot, S., and Guille, E. Differences in the consequences of the decay of radioactive <sup>64</sup>Cu atoms incorporated in cells under either *in vitro* or *in vivo* conditions. *Radiat. Environ. Biophys.*, *26*: 115–123, 1987.
64. Anderson, C., Dehdashti, F., Cutler, P., Schwarz, S., Laforest, R., Bass, L., Lewis, J., and McCarthy, D. Copper-64-octreotide as a PET imaging agent for patients with neuroendocrine tumors. *J. Nucl. Med.*, *42*: 213–221, 2001.
65. Philpott, G., Schwarz, S., Anderson, C., Dehdashti, F., Connet, J., Zinn, K., Mearns, C., Cutler, P., Welch, M., and Siegel, B. RadioimmunPET: detection of colorectal carcinoma with positron emitting copper-64-labeled monoclonal antibody. *J. Nucl. Med.*, *36*: 1818–1824, 1995.
66. Pohlit, W., and Harder, D. The shape of dose-survival curves for mammalian cells and repair of potentially lethal damage analyzed by hypertonic treatment. *Radiat. Res.*, *87*: 613–634, 1981.
67. Barendsen, G. Differences between biological effects of high LET and low LET radiations in relation to their application in radiotherapy. *Radiol. Clin.*, *46*: 380–389, 1977.
68. Ostashevsky, J. prediction of cell survival curves from DNA double-stranded break repair for low and high LET radiation. *Int. J. Radiat. Biol.*, *56*: 999–1010, 1989.
69. Clavo, A., Brown, R., and Wahl, R. Fluorodeoxyglucose uptake in human cancer cells is increased by hypoxia. *J. Nucl. Med.*, *36*: 1625–1632, 1995.
70. Aloj, L., Caraco, C., Jagoda, E., Eckelman, W., and Neumann, R. Glut-1 and hexokinase expression: relationship with 2-fluoro-2-deoxy-D-glucose uptake in A431 and T47D cells in culture. *Cancer Res.*, *59*: 4709–4714, 1999.
71. Burgman, P., O'Donoghue, J., Humm, J., and Ling, C. Hypoxia-induced increase in FDG uptake in MCF7 cells. *J. Nucl. Med.*, *42*: 170–175, 2001.
72. Hamilton, E., Fennell, M., and Stafford, D. Modification of tumor glucose metabolism for therapeutic benefit. *Acta Oncol.*, *34*: 429–433, 1995.
73. Lichter, A., and Lawrence, T. Recent advances in radiation oncology. *N. Engl. J. Med.*, *332*: 371–379, 1995.
74. Jha, B., and Pohlit, W. Reversibility of inhibition of DNA double strand break repair by 2-deoxy-D-glucose. *Int. J. Radiat. Biol.*, *63*: 459–467, 1993.
75. Jain, V., Kalia, V., Sharma, R., Maharajan, V., and Menon, M. Effects of 2-deoxy-D-glucose on glycolysis, proliferation kinetics and radiation response of human cancer cells. *Int. J. Radiat. Oncol. Biol. Phys.*, *11*: 943–950, 1985.
76. Gaze, M. The current status of targeted radiotherapy in clinical practice. *Phys. Med. Biol.*, *41*: 1895–1903, 1996.